

Memory Analysis for Memristors and Memristive Recurrent Neural Networks

Gang Bao, *Member, IEEE*, Yide Zhang, *Student Member, IEEE*, and Zhigang Zeng, *IEEE Fellow*

Abstract—Traditional recurrent neural networks are composed of capacitors, inductors, resistors, and operational amplifiers. Memristive neural networks are constructed by replacing resistors with memristors. This paper focuses on the memory analysis, i.e. the initial value computation, of memristors. Firstly, we present the memory analysis for a single memristor based on memristors' mathematical models with linear and nonlinear drift. Secondly, we present the memory analysis for two memristors in series and parallel. Thirdly, we point out the difference between traditional neural networks and those that are memristive. Based on the current and voltage relationship of memristors, we use mathematical analysis and SPICE simulations to demonstrate the validity of our methods.

Index Terms—Dopant drift, memory, memristive neural networks, memristor.

I. INTRODUCTION

THE memristor was first defined by Chua [1] and can be described by the following mathematical model [2]

$$\begin{cases} \frac{dx(t)}{dt} = f(x(t), u(t), t) \\ y(t) = g(x(t), u(t), t)u(t) \end{cases} \quad (1)$$

where $u(t)$, $y(t)$ are input and output of memristive systems, respectively. $x(t)$ is the state variable, $f(x(t), u(t), t)$ is a n -dimensional vector function and $g(x(t), u(t), t)$ is the generalized system response. Williams and his colleagues transform the concept of memristors into the physical devices [3], whose structure diagram is shown in Fig. 1. The memristor is com-

Manuscript received August 9, 2019; accepted October 24, 2019. The work was supported by the National Natural Science Foundation of China (61876097, 61673188, 61761130081), the National Key Research and Development Program of China (2016YFB0800402), the Foundation for Innovative Research Groups of Hubei Province of China (2017CFA005), and the Fundamental Research Funds for the Central Universities (2017KFXXJC002). Recommended by Associate Editor Yanjun Liu. (*Corresponding author: Gang Bao.*)

Citation: G. Bao, Y. D. Zhang, and Z. G. Zeng, "Memory analysis for memristors and memristive recurrent neural networks," *IEEE/CAA J. Autom. Sinica*, vol. 7, no. 1, pp. 96–105, Jan. 2020.

G. Bao is with Hubei Key Laboratory of Cascaded Hydropower Stations Operation and Control, Electrical Engineering and New Energy, China Three Gorges University, Yichang 443002, and Hubei Key Laboratory of Applied Mathematics (Hubei University), Wuhan 430074, China (e-mail: ctgugangbao@ctgu.edu.cn).

Y. D. Zhang is with Andrew and Peggy Cherg Department of Medical Engineering, California Institute of Technology, Pasadena, California 91125 USA (e-mail: yzhang34@nd.edu).

Z. G. Zeng is with the School of Artificial Intelligence and Automation, Huazhong University of Science and Technology, and also with the Key Laboratory of Image Processing and Intelligent Control of Education Ministry of China, Wuhan 430074, China (e-mail: zgzeng@hust.edu.cn).

Color versions of one or more of the figures in this paper are available online at <http://ieeexplore.ieee.org>.

Digital Object Identifier 10.1109/JAS.2019.1911828

posed of a two-layer TiO_2 thin film, two platinum contacts, a doped region R_{on} , and an undoped region R_{off} . D , w are the thickness of the film and the width of the doped region, respectively. Later, Chua points out that all two-terminal non-volatile memory devices based on resistance switching are memristors, regardless of the device material and physical operating mechanisms [4].

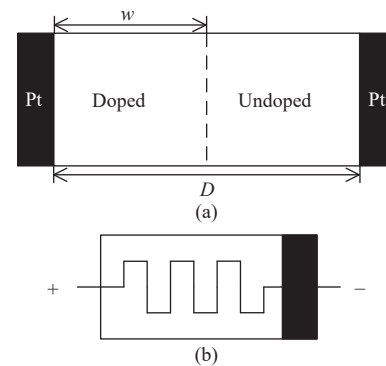


Fig. 1. The schematic diagram of the HP memristor. (a) The diagram of the HP memristor model. (b) The circuit symbol of the memristor, showing the positive and negative polarities.

The memristor has various applications for its nano-scale size and memory property. For example, it is used to implement chaotic circuits [5], [6], memristor oscillators [7], and neural synapses [8]. Snider *et al.* adopt memristors in neuromorphic applications to simulate learning, adaptive and spontaneous behaviors and to implement synaptic weights in artificial neural networks [9], [10]. Pershin and Di Ventra give an experimental demonstration for associative memory with memristive neural networks [11]. Then the memristor is employed as a nonvolatile memory storage device [12], [13]. Furthermore, it has also been used to simulate the human brain's hierarchical temporal memory, short-term, long-term memory [14], [15] and memristive recurrent neural networks. Meanwhile, memristors have also been harnessed for image processing, adaptive filters, digital logic, neuromorphic engineering, digital and quantum computation [16], [17], etc.

The dynamic properties of memristors are the foundation for its applications; thus memristors with different materials and configurations are made for dynamic analysis experiments [18], [19]. Williams *et al.* [3] present the mathematical model for memristors and show its fingerprint characteristic with a pinched hysteresis current i -voltage v loop. Based on Williams' mathematical model of memristors, Wang [20] derives the formula of the internal state $x(t)$ and obtains the analytical

expression of the current $i(t)$ and the voltage $v(t)$. Considering the doped materials' nonlinear drift, Biolek *et al.* [21] introduce window functions and give the SPICE model of memristors. Using Bernoulli dynamics, Drakakis *et al.* [22] derive the analytic description, $I_{\text{mres}} = f(V_{\text{mres}})$ which defines the relation between the current I_{mres} and the voltage V_{mres} under the assumption of nonlinear dopant drift. Wang *et al.* [23] and Zhang *et al.* [24] propose a piecewise linear (PWL) memristance model for studying dynamic properties of memristors. For single memristors, Biolek *et al.* [25], [26] demonstrate a methodology to obtain the analytical solution of a memristor's voltage/current response under the current/voltage excitation. For the properties of multiple memristors, Bao *et al.* [27] give the voltage-current relationship of parallel memristors. Kim *et al.* [28], [29] analyze the composite behavior of multiple connected memristors under the assumption that all memristors should reach a stable state. Then they construct a memristor emulator which could be connected in serial, parallel, or hybrid, simplifying the study of multiple memristors.

The memristive recurrent neural networks (MRNNs) are presented by replacing linear resistors with memristors in classical recurrent neural networks circuits. There are some compound results about the dynamical characteristics of the MRNNs [30]–[33]. Furthermore, we found that the MRNNs are a family of neural networks [34]. The MRNNs can be region stable and convergent to a sub neural network in the family of neural networks. Such a convergent result is dependent on the initial values of memristive synapses and network states. Hence, it is important to locate the initial states of memristive synapses and analyze the memory property of memristors. Although memory analysis has been discussed in the existing literature, determining how to locate the state of a memristor is scarcely discussed. With this motivation, we investigate the memory property of a memristor based on the relation between its voltage $v(t)$ and current $i(t)$ and give the method to locate the initial states of the memristive synapses. Our analysis comprehensively includes memristors under the assumptions of both linear and nonlinear dopant drift. We also extend the methods to obtain the initial states of two memristors connected in series and parallel, whose initial states can be obtained simultaneously with only a few measurements and one integration. SPICE simulations have been conducted for each presented method. The simulation results convincingly confirm the viability of our approaches. The rest of this paper is organized as follows: in Section II, we analyze the memory property of the memristor with linear and nonlinear dopant drift under a current and a voltage source, respectively. Further discussion on the memory property of two series- or parallel-connected memristors, as well as the algorithm to locate the initial states of memristive synapses, are provided in Section III. Finally, Section IV concludes the paper.

II. MEMORY ANALYSIS FOR ONE MEMRISTOR

In this section, we discuss a method to compute the initial value of a single memristor under voltage and current sources by using the memristor models with linear and nonlinear dopant drift.

A. Linear Dopant Drift With Current Excitation

In this section, we consider the memory of single memristive synapses based on Williams's memristor model [3] as follows:

$$v(t) = \left(R_{\text{on}} \frac{w(t)}{D} + R_{\text{off}} \left(1 - \frac{w(t)}{D} \right) \right) i(t) \frac{dw(t)}{dt} = \mu_V \frac{R_{\text{on}}}{D} i(t) \quad (2)$$

where $i(t)$, μ_V are the current through the device and the average ionic mobility, respectively; $v(t)$ is the applied voltage source. Let $x(t) = w(t)/D$ be the state variable of the memristor, as in (1); then, (2) can be rewritten as

$$v(t) = (R_{\text{on}}x(t) + R_{\text{off}}(1 - x(t)))i(t) \frac{dx(t)}{dt} = \mu_V \frac{R_{\text{on}}}{D^2} i(t) \quad (3)$$

with $x(t) \in [0, 1]$. Let $M(t) = R_{\text{on}}x(t) + R_{\text{off}}(1 - x(t))$. A pinched hysteresis loop figure, the fingerprint characteristic of the memristor, can be obtained by applying a sinusoidal current source $i(t) = i_0 \sin(\omega t)$ to the memristor. An HSPICE simulation is conducted and the result is shown in Fig. 2. The simulation parameters are set as following: $i_0 = 200 \mu\text{A}$, $\omega = 2\pi \text{ rad/s}$, $x(t_0) = 0.1$, $t_0 = 0 \text{ s}$, $R_{\text{on}} = 100\Omega$, $r = R_{\text{off}}/R_{\text{on}} = 160$, $D = 10^{-6} \text{ cm}$, $\mu_V = 10^{-10} \text{ cm}^2/\text{Vs}$.

Remark 1: From (2) and (3), the memristance is variable in the interval $[R_{\text{on}}, R_{\text{off}}]$. The memristance will be changed when the voltage or the current source is applied to the device. The

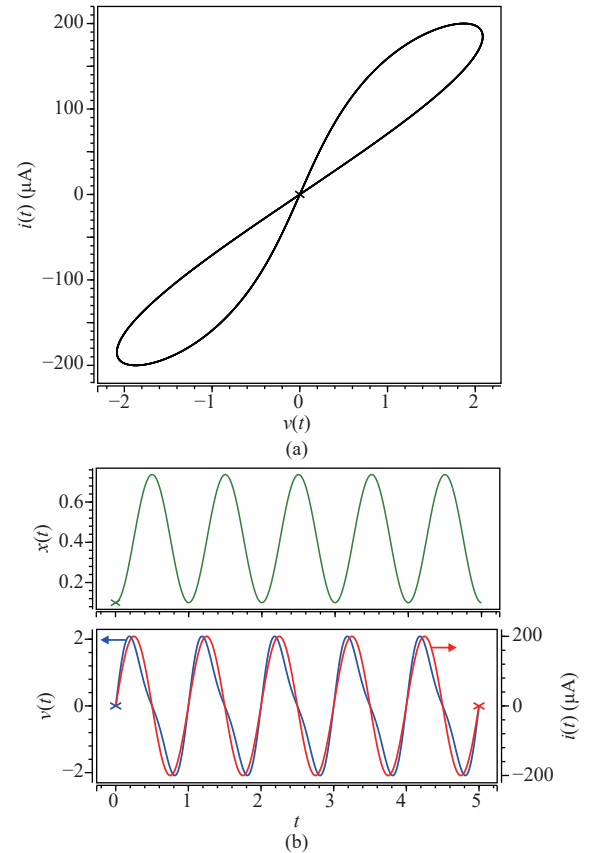


Fig. 2. The dynamical characteristics of the linear HP memristor. (a) The linear memristor's fingerprint characteristic: pinched hysteresis loop figure. (b) The change of the state $x(t)$, applied current source $i(t)$ and the corresponding voltage $v(t)$ of the memristor.

initial value of the memristor is the memristance $M(t_0) = R_{\text{on}}x(t_0) + R_{\text{off}}(1 - x(t_0))$ before the voltage or the current source is applied. The initial value can be memorized by the memristor and it affects memristance variation. This point, however, has not been discussed in the literature. The simulation parameters are chosen by using those in [3]. We compute the initial state of the memristor with the voltmeter-ammeter method and consider two cases, i.e., current excitation and voltage excitation, as shown in Fig. 3. The developed methods are for linear and nonlinear dopant drift.

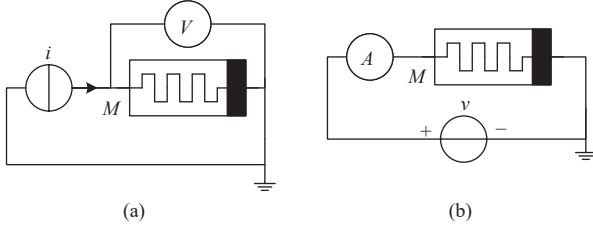


Fig. 3. Circuits for measuring the initial state of a memristor, under the excitation of (a) a current source and (b) a voltage source. V and I are voltmeter and ammeter, respectively.

Let $\xi = \mu_V \frac{R_{\text{on}}}{D^2}$, then we get

$$\frac{dx(t)}{dt} = \xi i(t) \quad (4)$$

and

$$i(t) = \frac{1}{\xi} \frac{dx(t)}{dt}. \quad (5)$$

We apply a current source at time $t = t_0$ and let $q(t) = \int i(t)dt$, $q(t_0) = 0$. Then we integrate both sides of (5) for $\forall t > t_0$, thus we have

$$\begin{aligned} \int_{t_0}^t i(s)ds &= \frac{1}{\xi} \int_{t_0}^t \frac{dx(s)}{ds} ds \\ q(t) &= \frac{1}{\xi} (x(t) - x(t_0)) \end{aligned} \quad (6)$$

and

$$x(t) = \xi q(t) + x(t_0). \quad (7)$$

Substituting (7) into (3),

$$v(t) = (R_{\text{off}} + (R_{\text{on}} - R_{\text{off}})(\xi q(t) + x(t_0)))i(t) \quad (8)$$

and then

$$x(t_0) = \frac{v(t) - R_{\text{off}}i(t)}{(R_{\text{on}} - R_{\text{off}})i(t)} - \xi q(t) \quad (9)$$

where $i(t)$ is the known current source, $q(t) = \int i(t)dt$, and $v(t)$ can be measured with a voltmeter. R_{off} , R_{on} , ξ are known parameters. Therefore we get the formula for the initial state of a memristor with linear dopant drift.

Next we verify this method with an HSPICE simulation. Predetermining $x(t_0)$ to be 0.28, we run the circuit in Fig. 3(a) for 2.73 s, while other parameters are the same with those in Fig. 2. The simulation process is presented in Fig. 4. After 2.73 s, the current $i(2.73)$ and voltage $v(2.73)$ across the memristor are $-198.4229 \mu\text{A}$ and -1.16128 V , respectively.

Since the current source is sinusoidal, we get $q(2.73) = 3.582 \times 10^{-5} \text{ C}$ by integrating $i(t)$ from $t = 0$ to $t = 2.73 \text{ s}$. Therefore we can apply the mathematical method and get $x(t_0) = 0.28$ which matches the value we predetermined. The result verifies that our method of applying current excitation to determine the initial state of a linear memristor is feasible.

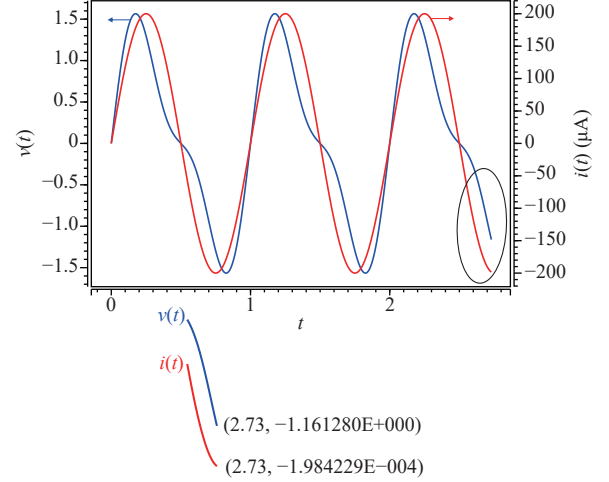


Fig. 4. Simulation process of a linear memristor under the current source for 2.73 s.

B. Linear Dopant Drift With Voltage Excitation

In this section, we consider the voltage excitation and drive the formula for $x(t_0)$. In (3), let $\beta = D^2/\mu_V$, and then

$$v(t) = \beta(x(t) + \frac{R_{\text{off}}}{R_{\text{on}}}(1 - x(t))) \frac{dx(t)}{dt}. \quad (10)$$

We apply a voltage source at time $t = t_0$ and let $\varphi(t) = \int v(t)dt$, $r = R_{\text{off}}/R_{\text{on}}$, and $\varphi(t_0) = 0$. Then we integrate both sides of (10) for $\forall t > t_0$,

$$\begin{aligned} \int_{t_0}^t v(s)ds &= \int_{t_0}^t \beta(x(s) + r(1 - x(s)))dx(s) \\ \varphi(t) &= \beta \left(\frac{1-r}{2} x^2(t) + rx(t) + c \right) \end{aligned} \quad (11)$$

where

$$c = \frac{r-1}{2} x^2(t_0) - rx(t_0). \quad (12)$$

It is easy to find that the constant c of the integration is dependent on initial value of $x(t)$ at $t = t_0$. Therefore the memory effect of memristors is attributed to the integration constant c . Next we deduce the analytic expression of $i(t)$ and $v(t)$. Since $x(t) \in [0, 1]$, from (11), we get

$$x(t) = \frac{r - \sqrt{r^2 + 2(r-1)\left(-\frac{\varphi(t)}{\beta} + c\right)}}{r-1}. \quad (13)$$

Differentiating (13) with respect to time t , then we obtain

$$\frac{dx(t)}{dt} = \frac{v(t)}{\beta \sqrt{r^2 + 2(r-1)\left(-\frac{\varphi(t)}{\beta} + c\right)}} \quad (14)$$

in which constant c is not removed. Based on (3), we have

$$i(t) = \frac{v(t)}{R_{\text{on}} \sqrt{r^2 + 2(r-1) \left(-\frac{\varphi(t)}{\beta} + c \right)}}. \quad (15)$$

From (15), we can obtain c by solving (15) with $i(t) \neq 0$ as

$$c = \frac{\left(\frac{v(t)}{R_{\text{on}} i(t)} \right)^2 - r^2}{2(r-1)} + \frac{\varphi(t)}{\beta}. \quad (16)$$

Then by (12), the initial state $x(t_0)$ can be obtained

$$\begin{cases} c = \frac{\left(\frac{v(t)}{R_{\text{on}} i(t)} \right)^2 - r^2}{2(r-1)} + \frac{\varphi(t)}{\beta} \\ x(t_0) = \frac{-r + \sqrt{r^2 + 2(r-1)c}}{1-r} \end{cases} \quad (17)$$

where $v(t)$ is the applied voltage source, $i(t)$ can be measured with an ammeter, r , R_{on} , β are known and $\varphi(t)$ can be calculated by $\varphi(t) = \int v(t) dt$. So $x(t_0)$ can be deduced from (17) if it is unknown.

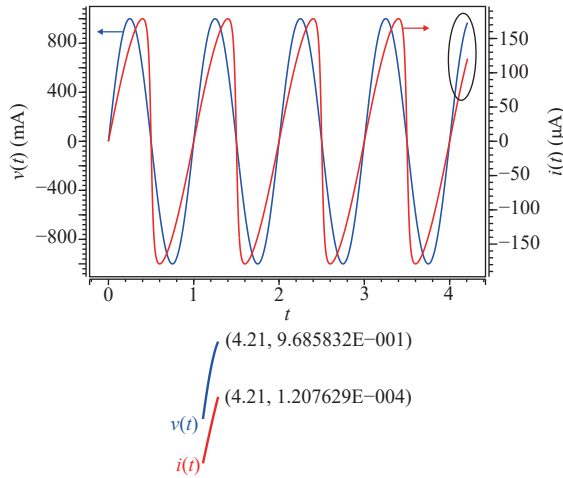


Fig. 5. Simulation process of a linear memristor under the voltage source for 4.21 s.

The result can be easily examined with a simulation. We simulate the circuit Fig. 3(b) on HSPICE. The initial state of the linear memristor is predetermined as 0.37. The applied voltage is a simple sinusoidal voltage source $v(t) = v_0 \sin(\omega t)$, where $v_0 = 1\text{V}$, $\omega = 2\pi \text{ rad/s}$. The other simulation parameters are set as following: $t_0 = 0 \text{ s}$, $R_{\text{on}} = 100\Omega$, $r = 160$, $D = 10^{-6} \text{ cm}$, $\mu_V = 10^{-10} \text{ cm}^2/\text{sV}$. We run the simulation for 4.21 s. At the end of the simulation, we get $v(4.21) = 968.5832 \text{ mV}$ and $i(4.21) = 120.7629 \mu\text{A}$. Because the applied voltage source is sinusoidal, $\varphi(t)$ can be calculated from the integration from $t = 0$ to $t = 4.21 \text{ s}$: $\varphi(4.21) = 0.1196 \text{ Wb}$. Thus we can apply the mathematical method in (17) and obtain

$$c = -48.3164, \quad x(t_0) = 0.37$$

which is the same with what we predetermined for $x(t_0)$. From the result, the viability of our method has been examined by

the simulation.

C. Nonlinear Dopant Drift With Current Excitation

In this section, we will show the methods to determine the initial state $x(t_0)$ of the memristor under the assumption of nonlinear dopant drift. For the nonlinear memristor, the descriptive model should be adjusted from (3) to

$$\begin{aligned} v(t) &= (R_{\text{on}} x(t) + R_{\text{off}}(1-x(t)))i(t) \\ \frac{dx(t)}{dt} &= \mu_V \frac{R_{\text{on}}}{D^2} i(t) f(x(t)) \end{aligned} \quad (18)$$

where $f(x(t))$ is a window function such that $f(0) = f(1) = 0$ ensures no drift at boundaries. The window function in model (18) is

$$f(x) = 1 - (2x - 1)^{2p} \quad (19)$$

in which p is a positive integer. $f(x)$ is shown in Fig. 6 for $p = 1, 2, 5$, respectively. As p increases, the curve get flatter in the middle and becomes steeper at the boundaries. If not specified, all nonlinear memristors are configured as $p = 1$ in the rest of this paper.

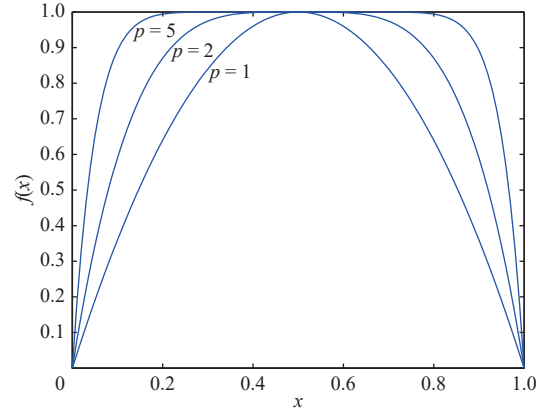


Fig. 6. Illustration for window function $f(x) = 1 - (2x - 1)^{2p}$ with $p = 1, 2, 5$.

Taking $p = 1$ in (19) and combing with (18), we get

$$\begin{aligned} v(t) &= (R_{\text{on}} x(t) + R_{\text{off}}(1-x(t)))i(t) \\ \frac{dx(t)}{dt} &= 4\mu_V \frac{R_{\text{on}}}{D^2} x(t)(1-x(t))i(t). \end{aligned} \quad (20)$$

The fingerprint characteristic of the memristor with nonlinear dopant drift, a bow-tie shape $i-v$ figure, can be generated by applying a sinusoidal current source $i(t) = i_0 \sin(\omega t)$ to the memristor. Based on (20), an HSPICE simulation is performed and the result is shown in Fig 7. The simulation parameters are set as following: $i_0 = 800 \mu\text{A}$, $\omega = 2\pi \text{ rad/s}$, $r = 160$, $D = 10^{-6} \text{ cm}$, $\mu_V = 10^{-10} \text{ cm}^2/\text{sV}$.

Let $\xi = \mu_V R_{\text{on}}/D^2$ and simplify (20) as

$$\frac{dx(t)}{dt} = 4\xi x(t)(1-x(t))i(t) \quad (21)$$

then

$$i(t) = \frac{1}{4\xi} \left(\frac{1}{x(t)} + \frac{1}{1-x(t)} \right) \frac{dx(t)}{dt}. \quad (22)$$

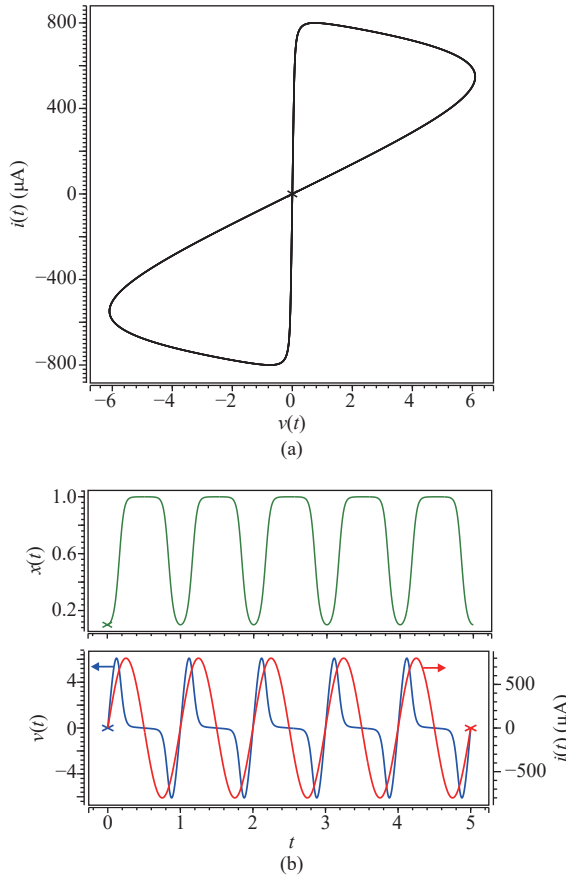


Fig. 7. The dynamical characteristics of the nonlinear HP memristor (a) The nonlinear memristor's fingerprint characteristic: bow-tie shape figure. (b) The change of the state $x(t)$, applied current source $i(t)$ and corresponding voltage $v(t)$ of a nonlinear memristor.

For the initial time t_0 , $q(t_0) = 0$, we integrate both sides of (22) for $\forall t > t_0$

$$\int_{t_0}^t i(s) ds = \frac{1}{4\xi} \int_{t_0}^t \left(\frac{1}{x(s)} + \frac{1}{1-x(s)} \right) dx(s) ds$$

$$q(t) = \frac{1}{4\xi} \left(\ln \frac{x(t)}{1-x(t)} - \ln \frac{x(t_0)}{1-x(t_0)} \right). \quad (23)$$

Let

$$c = \frac{x(t_0)}{1-x(t_0)} \quad (24)$$

and solve (23) for $x(t)$, we have

$$x(t) = \frac{ce^{4\xi q(t)}}{1+ce^{4\xi q(t)}}. \quad (25)$$

From (24), we can find the determinant relation between the constant c and $x(t_0)$. In other words, c includes the history information of $x(t)$. Now substitute (25) into (20), and we get

$$v(t) = \left(R_{\text{off}} + (R_{\text{on}} - R_{\text{off}}) \frac{ce^{4\xi q(t)}}{1+ce^{4\xi q(t)}} \right) i(t) \quad (26)$$

from which c can be calculated by

$$c = e^{-4\xi q(t)} \frac{v(t) - R_{\text{off}} i(t)}{R_{\text{on}} i(t) - v(t)}. \quad (27)$$

Therefore the initial state $x(t_0)$ of the nonlinear memristor is obtained by solving (24),

$$\begin{cases} c = e^{-4\xi q(t)} \frac{v(t) - R_{\text{off}} i(t)}{R_{\text{on}} i(t) - v(t)} \\ x(t_0) = \frac{c}{1+c} \end{cases} \quad (28)$$

where $i(t)$ is the current source, $q(t)$ can be calculated by $q(t) = \int i(t) dt$, $v(t)$ can be measured by the voltmeter, R_{off} , R_{on} , ξ are known. Thus with only a voltmeter and related calculation, the initial state of a memristor, under the assumption of nonlinear dopant drift, can be obtained.

The result of the HSPICE simulation agrees with the method. We preset $x(t_0) = 0.53$, and then run the circuit in Fig. 3(a) for 3.67 s. The parameters of the circuit are kept the same with those in Fig. 7. The simulation result is shown in Fig. 8. At the end of the simulation, the current $i(3.67)$ and voltage $v(3.67)$ of the memristor are $-701.0453 \mu\text{A}$ and -75.32032 mV , respectively. Because the current source is sinusoidal, we can calculate $q(3.67) = 1.8866 \times 10^{-4} \text{ C}$ by integrating $i(t)$ from $t = 0$ to $t = 3.67$ s. Therefore

$$c = 1.1277, \quad x(t_0) = 0.53.$$

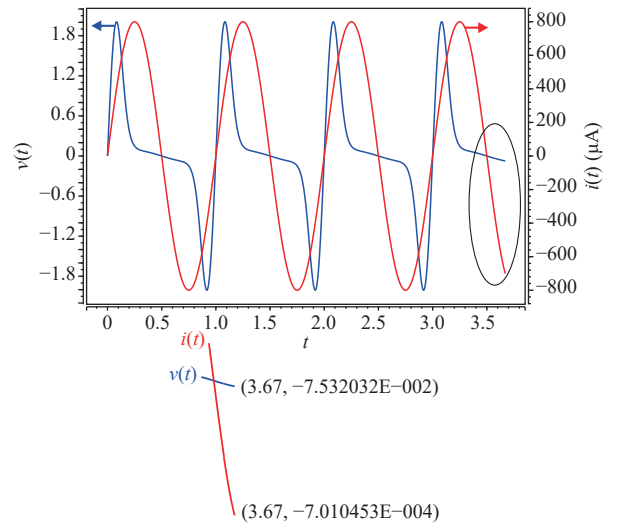


Fig. 8. Simulation process of a nonlinear memristor under the current source for 3.67 s.

The simulation result matches the value we predetermined for $x(t_0)$. That means the method is applicable for the calculation of initial states of memristors under the nonlinear dopant drift assumption.

D. Nonlinear Dopant Drift With Voltage Excitation

For nonlinear memristors, the initial state $x(t_0)$ can also be acquired through voltage excitation. From (20), we have

$$i(t) = \frac{\beta}{4R_{\text{on}}} \frac{1}{x(t)(1-x(t))} \frac{dx(t)}{dt} \quad (29)$$

where $\beta = D^2/\mu\nu$. Substitute $i(t)$ with (29) into (20), and we get

$$v(t) = \frac{\beta}{4} \left(\frac{1}{1-x(t)} + \frac{R_{\text{off}}}{R_{\text{on}}} \frac{1}{x(t)} \right) \frac{dx(t)}{dt}. \quad (30)$$

We apply the voltage source at $t = t_0$ and let $\varphi(t) = \int v(t)dt$, $r = R_{\text{off}}/R_{\text{on}}$, and $\varphi(t_0) = 0$. Then we integrate both sides of (30) for $\forall t > t_0$

$$\int_{t_0}^t v(s)ds = \frac{\beta}{4} \int_{t_0}^t \left(\frac{1}{1-x(s)} + r \frac{1}{x(s)} \right) \frac{dx(s)}{ds} ds$$

$$\varphi(t) = -\frac{\beta}{4} (\ln(1-x(t)) + r \ln x(t)) + \ln(1-x(t_0)) - r \ln x(t_0). \quad (31)$$

Let

$$c = \frac{x^r(t_0)}{1-x(t_0)} \quad (32)$$

then (31) can be simplified to

$$c e^{\frac{4\varphi(t)}{\beta}} = \frac{x^r(t)}{1-x(t)}. \quad (33)$$

The relation between c and $x(t_0)$ in (32) claims that the initial state of a nonlinear memristor can be calculated from the integration constant c . That is to say, the memory effect of nonlinear memristors can be represented by an integration constant. Next we deduce how to calculate c . Change (33) to

$$c = e^{-\frac{4\varphi(t)}{\beta}} \frac{x^r(t)}{1-x(t)} \quad (34)$$

where $v(t)$ is the applied voltage source, $i(t)$ can be measured with an ammeter, β and r are known, $\varphi(t)$ can be integrated from the applied voltage $v(t)$, and $\varphi(t) = \int v(t)dt$. The state $x(t)$ at time t can also be calculated from (20)

$$x(t) = \frac{v(t) - R_{\text{off}}i(t)}{(R_{\text{on}} - R_{\text{off}})i(t)}. \quad (35)$$

Combining (34) and (35), c is obtained by

$$c = e^{-\frac{4\varphi(t)}{\beta}} \left(\frac{v(t) - R_{\text{off}}i(t)}{(R_{\text{on}} - R_{\text{off}})i(t)} \right)^r \frac{(R_{\text{on}} - R_{\text{off}})i(t)}{R_{\text{on}}i(t) - v(t)}. \quad (36)$$

Then from (32), $x(t_0)$ can be acquired by solving an equation

$$x^r(t_0) + cx(t_0) - c = 0. \quad (37)$$

Since (37) is r -order, where r is undetermined, the analytical solution of $x(t_0)$ is not easy to get. So a numerical solution is recommended.

In order to get the numerical solution of $x(t_0)$, an algorithm is presented as follows. First, construct a function $z(x)$ according to (37)

$$z(x) = x^r + cx - c. \quad (38)$$

For $x(t_0) \in (0, 1)$, iterate $x(t_0)$ from 0 to 1, with a small increment δ (e.g., $\delta = 0.0001$) in each iteration. Notice that the precision of the numerical solution is dependent on δ : the smaller δ , the better the accuracy. During the iteration, $x(t_0)$ is regarded as the independent variable x to calculate $z(x)$ in (38). Since the derivative of $z(x)$

$$\frac{dz(x)}{dx} = rx^{r-1} + c > 0$$

$z(x)$ is monotonically increasing with the increment of x in every step. Continue the iteration until obtaining a \hat{x} such that $z(\hat{x}) > 0$, then compare the absolute value of $z(\hat{x})$ and $z(\hat{x} - \delta)$

to select the smaller one. As a result, the corresponding x to this smaller $z(x)$ is the numerical solution of $x(t_0)$ we are looking for.

An HSPICE simulation is conducted to verify this approach. The simulation circuit is the same with Fig. 3(b). Predetermining the initial state of the nonlinear memristor as 0.41, we apply a simple sinusoidal voltage source $v(t) = v_0 \sin(\omega t)$, where $v_0 = 1.2$ V, $\omega = 2\pi$ rad/s. The other simulation parameters are set as following: $t_0 = 0$ s, $R_{\text{on}} = 100 \Omega$, $r = 160$, $D = 10^{-6}$ cm, $\mu_V = 10^{-10}$ cm²/sV. The simulation lasted for 3.73 s and we get $v(3.73) = -1.190538$ V and $i(3.73) = -243.4537 \mu\text{A}$. Since the applied voltage source is sinusoidal, $\varphi(t)$ can be calculated from the integration from $t = 0$ to $t = 3.73$ s: $\varphi(3.73) = 0.2149$ Wb. Thus we can apply our mathematical method in (36)–(38) and obtain

$$c = 1.8818 \times 10^{-62}, \quad x(t_0) = 0.41.$$

The calculation result of $x(t_0)$ is the same with what we predetermined. The feasibility of our method has been examined from the simulation.

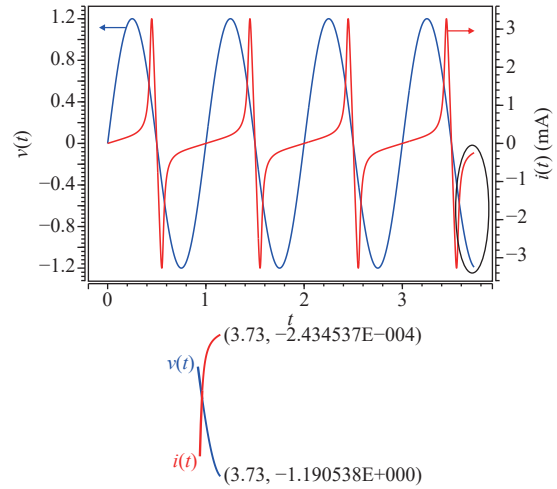


Fig. 9. Simulation process of a nonlinear memristor under the voltage source for 3.73 s.

Remark 2: From the analysis above, the integration constant c includes the information of the initial value $x(t_0)$. The memory is attributed to the integration constant c , which means that the initial value $x(t_0)$ can be computed by the integration constant c . For different models of the memristors, the formulas of the integration constant c are different. The accuracy of the initial value computation is dependent on the model of the device.

E. Memory Analysis for MRNNs

The model of the MRNNs is obtained by replacing linear resistors with memristors and can be described by the following differential systems

$$\dot{u}_i(t) = -\frac{u_i(t)}{R_i} + \sum_{j=1}^n \frac{f_j(u_j(t)) - u_i(t)}{M_{ij}(t)} + I_i \quad (39)$$

where $u_i(t)$, $i = 1, 2, \dots, n$, are the states of the network, $R_i, M_{ij}(t)$, $i, j = 1, 2, \dots, n$, are linear resistances and mem-

distances, respectively; $f_j(s)$ and I_i , $i, j = 1, 2, \dots, n$, $s \in \mathbb{R}$ are activation functions and bias currents, respectively.

According to the property of memristor, MRNNs are a cluster of neural networks. When the power is off, MRNNs can store their historic state. In order to analyze their memory property, i.e., computing initial values of every memristors, we use Algorithm 1 for the memory analysis for MRNNs.

Algorithm 1 Memory analysis for MRNNs

For the MRNNs with n^2 memristive synapses M_{ij} , $x_{ij}(t_0)$, $i, j = 1, 2, \dots, n$ represent the initial states of n^2 memristive synapses, and $u_i(t)$ $i = 1, 2, \dots, n$ are voltage values, and the states of MRNNs.

1. Derive analytical expressions of $u_i(t)$ $i = 1, 2, \dots, n$ with (39);
 2. Compute $f(u_j(t)) - u_i(t)$, for $i, j = 1, 2, \dots, n$ for some time t ;
 3. Use the above developed voltmeter-ammeter method to obtain $x_{ij}(t_0)$, $i, j = 1, 2, \dots, n$.
-

Remark 3: From (39), coefficients of MRNN are variable in the interval $[1/R_{\text{off}}, 1/R_{\text{on}}]$. If the MRNN can be convergent to one sub-network, the convergent result is dependent on the initial value $u_i(t_0)$ of the network state and the initial value $M_{ji}(t_0)$ of memristive synapses. It is necessary for us to locate the initial state of memristive synapses, i.e., analyzing the memory property of the memristor. It is difficult to obtain an accurate value of the voltage between two terminals of memristors. In future works, we will design suitable observers to obtain the voltage value of memristors. Memristors are nano-scale nonlinear resistors with stationary R_{on} and R_{off} . In practical applications, we need to connect two or more memristors in series or parallel to obtain different memristors with different memristances. Therefore, it is necessary to analyze the memory of two or more memristors in series or parallel.

III. MEMORY PROPERTIES OF TWO MEMRISTORS INTERCONNECTION

In this section, we will discuss memory properties of two series and parallel memristors. As discussed in Section II, one measurement value ($i(t)$ or $v(t)$) and one integration value ($q(t)$ or $\varphi(t)$) is needed to determine the initial state of the memristor. However, we do not need to conduct two measurements and two integrations for two memristors when they are connected in series or parallel, because the memristors connected in series share the same current, and the ones in parallel share the same voltage. Our approach is valid for n ($n > 1$) memristors connected in series and parallel: for the series connection case, n measurements for n individual voltages and an integration for the common charge are required; for the parallel connection case, we need n measurements for n individual currents and an integration for the shared magnetic flux. For the purpose of simplicity and without loss of generality, we only discuss two series and parallel memristors.

A. Two Memristors in Series

Firstly we discuss the memory property of two memristors M_1 and M_2 in series and discuss the method in finding initial

states of M_1 and M_2 . Denote $x_1(t_0)$, $x_2(t_0)$ as initial states of M_1 and M_2 . Then one can attach a given current source $i(t)$ to them and measure the corresponding voltage $v_1(t)$, $v_2(t)$ of M_1 , M_2 . When two memristors are connected in series, we should consider the memristors' polarities as shown in Fig. 10. In the situation of Fig. 10(a), M_1 and M_2 connected in series share the same polarity with the current source and voltmeters. We can directly apply (28) in Section II to each memristor. In Fig. 10(b), while M_1 shares the same polarity with the excitation, M_2 is opposite to the current source. Hence calculation methods for the initial state of M_2 should be adjusted. A negative sign should be added to $i(t)$, $v(t)$ and $q(t)$ to offset the polarity difference of M_2 . Since the existence of opposite polarity is more universal for series connected memristors, in this subsection, we only discuss the situation in Fig. 10(b).

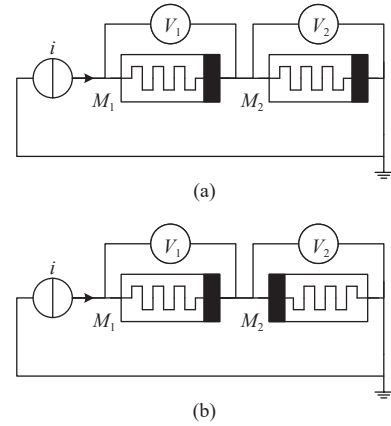


Fig. 10. Two memristors in series with (a) the same polarity and (b) the opposite polarity.

If the discussed memristors are under the assumption of linear dopant drift, we calculate the integration constant c_1 and the initial state $x_1(t_0)$ of M_1 . For M_2 , the memristor opposite to the one connected,

$$\begin{cases} \bar{c} = \frac{-v(t) + R_{\text{off}}i(t)}{(R_{\text{off}} - R_{\text{on}})i(t)} + \xi q(t) \\ \bar{x}(t_0) = c \end{cases} \quad (40)$$

where \bar{c} and $\bar{x}(t_0)$ are the integration constant and the initial state of a memristor connected in opposite polarity, respectively. So c_2 and $x_2(t_0)$ of M_2 can be obtained following (40).

An HSPICE simulation is conducted to examine this method for linear memristors in series. We predetermine the initial states $x_1(t_0)$, $x_2(t_0)$ to be 0.15 and 0.75, respectively. The simulation circuit is Fig. 10(b), where the current source $i(t) = i_0 \sin(\omega t)$, $i_0 = 200 \mu\text{A}$, and $\omega = 2\pi \text{ rad/s}$. The other simulation parameters are the same as the ones in Section II: $t_0 = 0 \text{ s}$, $R_{\text{on}} = 100 \Omega$, $r = 160$, $D = 10^{-6} \text{ cm}$, $\mu_V = 10^{-10} \text{ cm}^2/\text{sV}$. We then run the circuit for 3.13 s. $i(3.13) = 145.7937 \mu\text{A}$, $v_1(3.13)$ and $v_2(3.13)$ are measured as 1.752215 V and 826.8759 mV, respectively. Since the current source is sinusoidal, we get $q(3.13) = 1.0041 \times 10^{-5} \text{ C}$ by integrating $i(t)$ from $t = 0$ to $t = 3.13 \text{ s}$. With the presence of $i(3.13)$, $v_k(3.13)$

and $q(3.13)$, $k = 1, 2$, the initial states of M_1 , M_2 are obtained according to (40),

$$c_1 = 0.15, \quad x_1(t_0) = 0.15, \quad c_2 = 0.75, \quad x_2(t_0) = 0.75.$$

The results are coincident with the values we preset for $x_1(t_0)$, $x_2(t_0)$, representing the validity of the methods (40).

For series connected memristors under the assumption of nonlinear dopant drift, the integration constant c_1 and the initial state $x_1(t_0)$ of M_1 can be calculated from (28). As for the opposite connected M_2 , (28) should be adjusted to

$$\begin{cases} \bar{c} = e^{A\xi q(t)} \frac{-v(t) + R_{\text{off}}i(t)}{-R_{\text{on}}i(t) + v(t)} \\ \bar{x}(t_0) = \frac{\bar{c}}{1 + \bar{c}}. \end{cases} \quad (41)$$

Hence c_2 and $x_2(t_0)$ of M_2 can be obtained from (41).

This approach for series connected memristors with the nonlinear dopant drift can also be verified with an HSPICE simulation. We preset the initial states $x_1(t_0)$, $x_2(t_0)$ to be 0.21 and 0.47, respectively. The simulation circuit and parameters are identical to the ones above for linear memristors, except the magnitude of the current source is $i_0 = 800 \mu\text{A}$. Run the circuit for 4.11 s. At the end of the simulation, $i(4.11) = 509.9392 \mu\text{A}$, $v_1(4.11)$ and $v_2(4.11)$ are measured as 4.420901 V and 6.407382 V, respectively. Since the current source is sinusoidal, we can get $q(4.11) = 2.9219 \times 10^{-5} \text{C}$ by integrating $i(t)$ from $t = 0$ to $t = 4.11$ s. Now we have $i(4.11)$, $v_k(4.11)$ and $q(4.11)$, $k = 1, 2$, the initial states of M_1 , M_2 can be calculated according to (28) and (41)

$$c_1 = 0.2658, \quad x_1(t_0) = 0.21, \quad c_2 = 0.8868, \quad x_2(t_0) = 0.47.$$

The predetermined values for $x_1(t_0)$, $x_2(t_0)$ are obtained from the simulation, showing the feasibility of methods (28) and (41).

B. Two Memristors in Parallel

In this subsection, we study the property of two memristors in parallel and give the formulas to calculate the initial states of M_1 , M_2 . A common voltage source $v(t)$ is applied to them and the corresponding currents $i_1(t)$, $i_2(t)$ of M_1 , M_2 can be measured. When two memristors are connected in parallel, we should consider the memristors' polarities as shown in Fig. 11. In Fig. 11(a), M_1 and M_2 connected in parallel share the same polarity with the voltage source and the ammeters. Equations (17) or (36), and (37) in Section II can be applied to each memristor. In Fig. 11(b), however, M_2 is opposite to the voltage excitation, contrary to the regular connection of M_1 . Therefore the calculation methods for the initial state of M_2 should be adjusted accordingly. A negative sign is added to $v(t)$, $i(t)$ and $\varphi(t)$ to compensate for the polarity difference of M_2 . We only discuss the situation in Fig. 11(b) in this subsection, because the existence of opposite polarity is more general for parallel connected memristors.

First we discuss the memristors in parallel under the linear dopant drift assumption; the integration constant c_1 and the initial state $x_1(t_0)$ of M_1 can be calculated from (17). While c_2 and $x_2(t_0)$ of the opposite connected memristor M_2 can be obtained

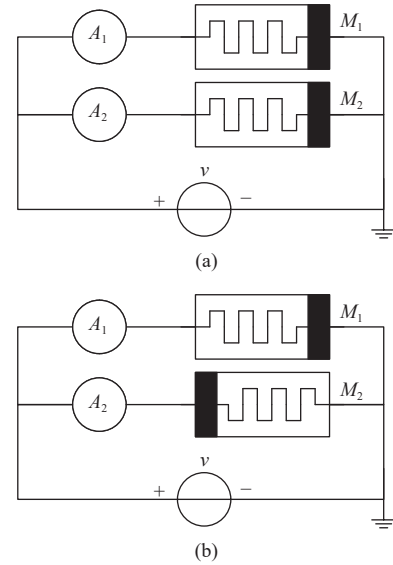


Fig. 11. Two memristors in parallel with (a) the same polarity and (b) the opposite polarity.

$$\begin{cases} \bar{c}_2 = \frac{\left(\frac{v(t)}{R_{\text{on}}i(t)}\right)^2 - r^2}{2(r-1)} - \frac{\varphi(t)}{\beta} \\ \bar{x}_2(t_0) = \frac{-r + \sqrt{r^2 + 2(r-1)c_2}}{1-r}. \end{cases} \quad (42)$$

A parallel memristors circuit simulation is conducted to examine this method. We preset the initial states $x_1(t_0)$, $x_2(t_0)$ to be 0.33 and 0.67, respectively. The simulation circuit is in Fig. 11(b), where the applied voltage is a simple sinusoidal voltage source $v(t) = v_0 \sin(\omega t)$, $v_0 = 1 \text{ V}$, $\omega = 2\pi \text{ rad/s}$. The other simulation parameters are the same with those in series connection. Run the simulation for 5.21 s. Then $v(5.21) = 968.5831 \text{ mV}$, $i_1(5.21)$ and $i_2(5.21)$ are measured as 109.9511 μA and 118.6726 μA , respectively. We can also get $\varphi(5.21) = 0.1196 \text{ Wb}$ by integrating $v(t)$ from $t = 0$ to $t = 5.21$ s since the voltage source is sinusoidal. With the existence of $v(5.21)$, $i_k(5.21)$ and $\varphi(5.21)$, $k = 1, 2$, the initial states of M_1 , M_2 are obtained according to (17) and (42),

$$c_1 = -44.1424, \quad x_1(t_0) = 0.33, \quad c_2 = -71.5125, \quad x_2(t_0) = 0.67.$$

The correctness of our approach is examined from the consistency of the result and preset values.

Then we should consider the situation when two memristors under the assumption of nonlinear dopant drift are connected in parallel. The integration constant c_1 of M_1 can be calculated from (36), and the initial state $x_1(t_0)$ can be obtained from solving (37). The numerical algorithm to determine the solution of (37) has been described in Section II-D. As for the opposite connected M_2 , (36) should be adjusted to

$$\bar{c} = e^{\frac{4\varphi(t)}{\beta}} \left(\frac{-v(t) + R_{\text{off}}i(t)}{(R_{\text{off}} - R_{\text{on}})i(t)} \right)^r \frac{(R_{\text{off}} - R_{\text{on}})i(t)}{-R_{\text{on}}i(t) + v(t)} \quad (43)$$

to get the integration constant c_2 of M_2 . And $x_2(t_0)$, the initial state of M_2 , can also be obtained from solving the equation

$$\bar{x}^r(t_0) + \bar{c}\bar{x}(t_0) - \bar{c} = 0. \quad (44)$$

We simulate the nonlinear memristors in parallel to test this

algorithm. Predetermining the initial states $x_1(t_0)$, $x_2(t_0)$ to be 0.45 and 0.54, respectively. The circuit and parameters are the same with the previous ones, except the magnitude of the voltage source $v_0 = 1.2$ V. The simulation is lasted for 5.77 s. At the end of the simulation, $v(5.77) = -1.190538$ V, $i_1(5.77)$ and $i_2(5.77)$ are measured as -230.0400 μ A and -115.2139 μ A, respectively. Since the voltage source is sinusoidal, we can calculate $\varphi(5.77) = 0.1670$ Wb by integrating $v(t)$ from $t = 0$ to $t = 5.77$ s. Now we get $v(5.77)$, $i_k(5.77)$ and $\varphi(5.77)$, $k = 1, 2$, the initial states of M_1 , M_2 can be obtained following the calculation of (36), (43) and the solution of (37), (44),

$$\begin{aligned} c_1 &= 5.7439 \times 10^{-56}, & x_1(t_0) &= 0.45 \\ c_2 &= 3.3133 \times 10^{-43}, & x_2(t_0) &= 0.54. \end{aligned}$$

The results are in accordance with the predetermined values.

Remark 4: For two memristors connected in series or parallel, the total initial memristance can be computed if the initial values $x_1(t_0)$, $x_2(t_0)$ are obtained, respectively. We focus on the memory analysis for two memristors in series or parallel, i.e., the total initial memristance computation. This is difference from the property analysis of two series or parallel memristors in the existing papers.

IV. CONCLUDING REMARKS

In this paper, we discuss the memory property of memristors by deriving the formula for the initial value formula and the voltmeter-ammeter method. Then we analyze two series and parallel memristors' memory. According to the developed memory analysis method, we give the algorithm for locating the initial values of all memristive synapses of the MRNN (39). Our analysis shows that the integration constant c in the expression plays an important role in the memory of the electronic device. The accuracy may be improved for the computation of the initial values if the state observer can be designed for the MRNN. This will be our future work.

REFERENCES

- [1] L. Chua, "Memristor—the missing circuit element," *IEEE Trans. Circ. Theory*, vol. 18, no. 5, pp. 507–519, 1971.
- [2] L. O. Chua and S. M. Kang, "Memristive devices and systems," *Proc. IEEE*, vol. 64, no. 2, pp. 209–223, 1976.
- [3] D. B. Strukov, G. S. Snider, D. R. Stewart, and R. S. Williams, "The missing memristor found," *Nature*, vol. 453, no. 7191, pp. 80–83, 2008.
- [4] L. Chua, "Resistance switching memories are memristors," *App. Phys. A*, vol. 102, no. 4, pp. 765–783, 2011.
- [5] M. Itoh and L. O. Chua, "Memristor oscillators," *Int. J. Bifurcation Chaos*, vol. 18, no. 11, pp. 3183–3206, 2008.
- [6] W. Sun, C. Li, and J. Yu, "A memristor based chaotic oscillator," in *Proc. Int. Conf. Com. Circ. Syst. (ICCCAS)*. IEEE, 2009, pp. 955–957.
- [7] T. Driscoll, Y. Pershin, D. Basov, and M. Di Ventra, "Chaotic memristor," *App. Phys. A*, vol. 102, no. 4, pp. 885–889, 2011.
- [8] B. Linares-Barranco and T. Serrano-Gotarredona, "Memristance can explain spike-time-dependent-plasticity in neural synapses," *Nature Prec.*, pp. 1–4, 2009.
- [9] G. Snider, "Memristors as synapses in a neural computing architecture," in *Memristor and Memristive Systems Symposium*, 2008.
- [10] G. Snider, "Self-organized computation with unreliable, memristive nanodevices," *Nanotechnology*, vol. 18, no. 36, pp. 365202, 2007.
- [11] Y. V. Pershin and M. Di Ventra, "Experimental demonstration of associative memory with memristive neural networks," *Neural Netw.*, vol. 23, no. 7, pp. 881–886, 2010.
- [12] T. Driscoll, H.-T. Kim, B.-G. Chae, B.-J. Kim, Y.-W. Lee, N. M. Jokerst, S. Palit, D. R. Smith, M. Di Ventra, and D. N. Basov, "Memory metamaterials," *Science*, vol. 325, no. 5947, pp. 1518–1521, 2009.
- [13] P. O. Vontobel, W. Robinett, P. J. Kuekes, D. R. Stewart, J. Straznicky, and R. S. Williams, "Writing to and reading from a nano-scale crossbar memory based on memristors," *Nanotechnology*, vol. 20, no. 42, pp. 425204, 2009.
- [14] K. Smagulova, O. Krestinskaya, and A. P. James, "A memristor-based long short term memory circuit," *Analog Integrated Circuits and Signal Processing*, vol. 95, no. 3, pp. 467–472, 2018.
- [15] A. Irmanova and A. P. James, "Neuron inspired data encoding memristive multi-level memory cell," *Analog Integrated Circuits and Signal Processing*, vol. 3, pp. 1–6, 2018.
- [16] Y. V. Pershin and M. Di Ventra, "Neuromorphic, digital, and quantum computation with memory circuit elements," *Proc. IEEE*, vol. 100, no. 6, pp. 2071–2080, 2012.
- [17] W. J.-S. S. J.-W. L. W. WANG Xiao-Ping, SHEN Yi, "Review on memristor and its applications," *Acta Automatica Sinica*, vol. 39, no. 8, pp. 1170, 2013.
- [18] Y. V. Pershin and M. Di Ventra, "Spin memristive systems: Spin memory effects in semiconductor spintronics," *Phys. Rev. B*, vol. 78, no. 11, pp. 113309, 2008.
- [19] I.-S. Yoon, J. S. Choi, Y. S. Kim, S. H. Hong, I. R. Hwang, Y. C. Park, S.-O. Kang, J.-S. Kim, and B. H. Park, "Memristor behaviors of highly oriented anatase TiO₂ film sandwiched between top Pt and bottom SrRuO₃ electrodes," *App. Phys. Express*, vol. 4, no. 4, pp. 1101, 2011.
- [20] F.-Y. Wang, "Memristor for introductory physics," arXiv Preprint arXiv: 0808.0286, 2008.
- [21] Z. Birolek, D. Birolek, and V. Biolková, "SPICE model of memristor with nonlinear dopant drift," *Radioengineering*, vol. 18, no. 2, pp. 210–214, 2009.
- [22] E. Drakakis, S. Yaliraki, and M. Barahona, "Memristors and Bernoulli dynamics," in *Proc. Int. Workshop Cell. Nano. Netw. App. (CNNA)*. IEEE, 2010, pp. 1–6.
- [23] D. Wang, Z. Hu, X. Yu, and J. Yu, "A PWL model of memristor and its application example," in *Proc. Int. Conf. Com. Circ. Syst. (ICCCAS)*. IEEE, 2009, pp. 932–934.
- [24] Y. Zhang, X. Zhang, and J. Yu, "Approximated SPICE model for memristor," in *Proc. Int. Conf. Com. Circ. Syst. (ICCCAS)*. IEEE, 2009, pp. 928–931.
- [25] Z. Birolek, D. Birolek, and V. Biolkova, "Analytical solution of circuits employing voltage- and current-excited memristors," *IEEE Trans. Circ. Syst.*, vol. 59, no. 11, pp. 2619–2628, 2012.
- [26] Z. Li, Y. Tao, A. Abu-Siada, M. A. S. Masoum, Z. Li, Y. Xu, and X. Zhao, "A new vibration testing platform for electronic current transformers," *IEEE Trans. Instrumentation and Measurement*, vol. 68, no. 3, pp. 704–712, 2019.
- [27] B. Bao, F. Feng, W. Dong, and S. Pan, "The voltage-current relationship and equivalent circuit implementation of parallel flux-controlled memristive circuits," *Chinese Phys. B*, vol. 6, pp. 101, 2013.
- [28] R. Budhathoki, M. Sah, S. Adhikari, H. Kim, and L. Chua, "Composite behavior of multiple memristor circuits," *IEEE Trans. Circ. Syst. I: Regular Papers*, vol. 60, no. 10, pp. 2688–2700, 2013.
- [29] H. Kim, M. Sah, C. Yang, S. Cho, and L. Chua, "Memristor emulator

for memristor circuit applications,” *IEEE Trans. Circ. Syst. I: Regular Papers*, vol. 59, no. 10, pp. 2422–2431, 2012.

- [30] G. Bao and Z. Zeng, “Stability analysis for memristive recurrent neural network under different external stimulus,” *Neural Processing Letters*, vol. 47, no. 2, pp. 601–618, 2018.
- [31] L. Wang, Z. Zeng, M.-F. Ge, and J. Hu, “Global stabilization analysis of inertial memristive recurrent neural networks with discrete and distributed delays,” *Neural Networks*, vol. 105, pp. 65–74, 2018.
- [32] L. Wang, T. Dong, and M.-F. Ge, “Finite-time synchronization of memristor chaotic systems and its application in image encryption,” *Applied Mathematics and Computation*, vol. 347, pp. 293–305, 2019.
- [33] Y. Sheng, H. Zhang, and Z. Zeng, “Stabilization of fuzzy memristive neural networks with mixed time delays,” *IEEE Trans. Fuzzy Systems*, vol. 26, no. 5, pp. 2591–2606, 2017.
- [34] G. Bao, Z. G. Zeng, and Y. J. Shen, “Region stability analysis and tracking control of memristive recurrent neural network,” *Neural Networks*, vol. 98, no. 2, pp. 51–58, 2018.



China Three Gorges University.

Gang Bao (M’19) received the B.S. degree in mathematics from Hubei Normal University, Huangshi, China, the M.S. degree in applied mathematics from Beijing University of Technology, Beijing, China, in 2000 and 2004, the Ph.D. degree from the Department of Control Science and Engineering, Huazhong University of Science and Technology, respectively. Now he is working at Hubei Key Laboratory of Cascaded Hydropower Stations Operation and Control Electrical Engineering and New Energy School,



Yide Zhang (S’13) received the B.E. degree in automation from Huazhong University of Science and Technology, China, in 2014, and the Ph.D. degree in electrical engineering from the University of Notre Dame, USA, in 2019. He is currently a Postdoctoral Scholar with the California Institute of Technology. His research is interdisciplinary and focused on developing new types of optical imaging techniques that could advance the work of other researchers and medical personnel in a wide variety of fields. His research interests include multiphoton microscopy, fluorescence lifetime imaging microscopy, super-resolution microscopy, photoacoustic tomography, high-speed imaging, deep tissue imaging, adaptive optics, computational imaging, and deep learning.



Zhigang Zeng (F’20) received the Ph.D. degree in systems analysis and integration from Huazhong University of Science and Technology, Wuhan, China, in 2003. He is currently a Professor with the School of Artificial Intelligence and Automation, Huazhong University of Science and Technology, Wuhan, China, and also with the Key Laboratory of Image Processing and Intelligent Control of the Education Ministry of China, Wuhan, China. He has been an Associate Editor of the *IEEE Transactions on Neural Networks* (2010 – 2011), *IEEE Transactions on Cybernetics* (since 2014), *IEEE Transactions on Fuzzy Systems* (since 2016), and a member of the Editorial Board of *Neural Networks* (since 2012), *Cognitive Computation* (since 2010), *Applied Soft Computing* (since 2013). He has published over 200 international journal papers. His current research interests include theory of functional differential equations and differential equations with discontinuous right-hand sides, and their applications to dynamics of neural networks, memristive systems, and control systems.